and the lifetime (less than the resolving time of the coincidence circuit, 2×10^{-6} second) of the 0.0574-Mev transition are all consistent with an $M1$ interpretation. Lack of exact theoretical values for α_K does not permit exclusion of some $E2$ admixture, but the lack of an observable L_{II} conversion line limits this possibility to a few percent.

The measured K/L ratio of the 0.294-Mev transition indicates several possibilities. $M3$ can be excluded because the life of this state is also less than the resolving time of the coincidence circuit. $M2$ or $E1$ interpretations are inconsistent with the plus parity of the 0.351-Mev state indicated by the beta-ray measurements. The remaining choice is $E2$.

According to the single-particle model, the ground state of Pr^{143} (59 neutrons) may be $d_{5/2}$ or $g_{7/2}$. Either assignment is consistent with the observed character of the beta transition to Nd^{143}, which has a measured spin[6] of 7/2 and is $f_{7/2}$ (83 neutrons). The ground state of Ce^{143} (85 neutrons) may be $f_{7/2}$ or $h_{9/2}$. The $f_{7/2}$ assignment is unsatisfactory since the state could then undergo a first-forbidden beta transition equally well to either of the possible choices for the ground state of Pr^{143}, whereas the ground-state transition is not observed. If it were $h_{9/2}$, however, decay to a $g_{7/2}$ state in Pr is only first forbidden, but decay to a $d_{5/2}$ state is "l-forbidden" with $\Delta l=3$. This assignment is therefore consistent with observation, if the Pr^{143} ground state is identified as $d_{5/2}$. Then the 0.0574-Mev excited level can be $g_{7/2}$, consistent with the $M1$ character of the gamma transition.

Although it is indicated above that the 0.294-Mev transition appears to be $E2$, the fact that the 0.351-Mev crossover is seen makes it seem unlikely that the 0.351-Mev level has a spin as great as 11/2. It is tentatively suggested that this is a $g_{9/2}$ state, and that there may be some $M1$ admixture in the 0.294-Mev transition.

V. ACKNOWLEDGMENTS

Thanks are expressed to Dr. J. M. LeBlanc and Dr. E. L. Church for many valuable discussions.

PHYSICAL REVIEW VOLUME 101, NUMBER 1 JANUARY 1, 1956

Magnetic Spectrograph Measurements on the $Al^{27}(d,p)Al^{28}$ Reaction*

W. W. BUECHNER, M. MAZARI,† AND A. SPERDUTO
Physics Department and Laboratory for Nuclear Science, Massachusetts Institute of Technology, Cambridge, Massachusetts
(Received July 12, 1955)

A broad-range magnetic spectrograph has been used to study the proton groups from $Al^{27}(d,p)Al^{28}$. In the region of excitation between the ground state and the neutron binding in Al^{28}, one hundred well-resolved groups were observed and assigned to this reaction on the basis of studies at bombarding energies of 6 and 7 Mev and at several angles of observation. The energy resolution of the proton groups ranged from 800 to 1600.

I. INTRODUCTION

ONE of the most active fields in present nuclear research is the investigation of the excited states of nuclei. An important method for such investigations is the study of the charged particles emitted from artificially produced nuclear reactions. The requirements for resolution and accuracy in this field are such that these studies are now commonly carried out with magnetic or electrostatic deflection of both the bombarding and the emitted particles.

In general, the magnetic or electric analyzers used can be classed as spectrometers, since they focus the charged particles onto a slit and electrical detection is used. A high-resolution study of a particle spectrum with such a spectrometer requires a point-by-point study of the number of particles through a narrow slit as a function of field strength. In a few cases, magnetic analyzers have been constructed with a geometry such that photographic detection can be employed to record a portion of the spectrum of charged particles. Such a magnetic spectrograph has been in use in this Laboratory for a number of years. While the resolution and accuracy of this instrument have been satisfactory, it has been apparent that an analyzer more closely resembling an optical spectrograph would have many advantages. With such an instrument, which would record simultaneously a considerable fraction of the complete particle spectrum, uncertainties in the energies and relative intensities of the particle groups, which often arise because of target changes during long bombardments, would be considerably reduced. Also, in cases where the spectrum to be investigated consists of more than a few groups, the resolution which could be obtained in practice with such a spectrograph would be greater than would be practical with the more usual spectrometer instrument.

* This work has been supported in part by the joint program of the Office of Naval Research and the U. S. Atomic Energy Commission.
† On leave from the National University of Mexico.

A number of possible designs for such a spectrograph were considered, and in 1951 construction of an instrument incorporating a geometry suggested by K. T. Bainbridge was started by the Laboratory group. The spectrograph was completed early in 1954, and brief descriptions have been given of its design and performance.[1,2]

The present work was undertaken primarily as an investigation of the dispersion and resolution of the spectrograph when used for nuclear reaction studies. Because of the complexity of its spectrum, the $Al^{27}(d,p)Al^{28}$ reaction was chosen for these studies. In previous work in this Laboratory, using incident deuterons in the range of 2.0 Mev, the protons emitted from this reaction at 90 degrees to the incident beam were analyzed with a 180-degree magnetic spectrograph. Fifty proton groups were assigned to this reaction, corresponding to the ground state and forty-nine excited states of Al^{28} between 0 and 6.35-Mev excitation.[3] The large number of closely spaced levels found by Enge *et al.* make this reaction a particularly suitable one for the present purpose.

A second objective of the work was, in view of possible future angular distribution studies, to determine whether in the earlier work some levels in Al^{28} might not have been observed, either because of the low bombarding energies used or because the observation angle was limited to 90 degrees.

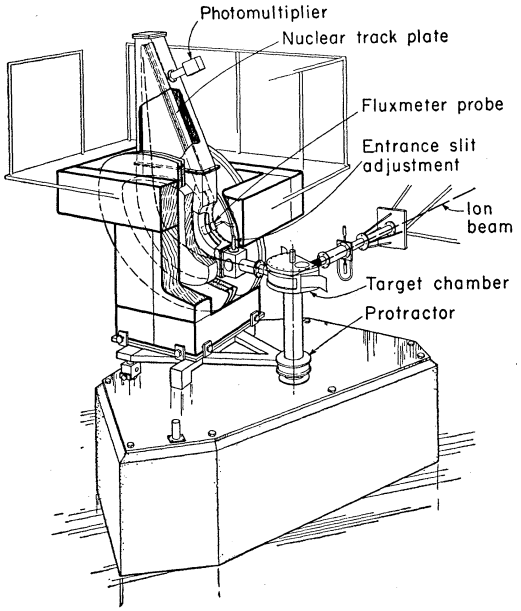

FIG. 1. Schematic diagram of broad-range magnetic spectrograph.

[1] Buechner, Browne, Enge, Mazari, and Buntschuh, Phys. Rev. **95**, 609 (1954).
[2] W. W. Buechner, *Proceedings of the 1954 Glasgow Conference on Nuclear and Meson Physics* (Pergamon Press, London, 1955).
[3] Enge, Buechner, and Sperduto, Phys. Rev. **88**, 963 (1952).

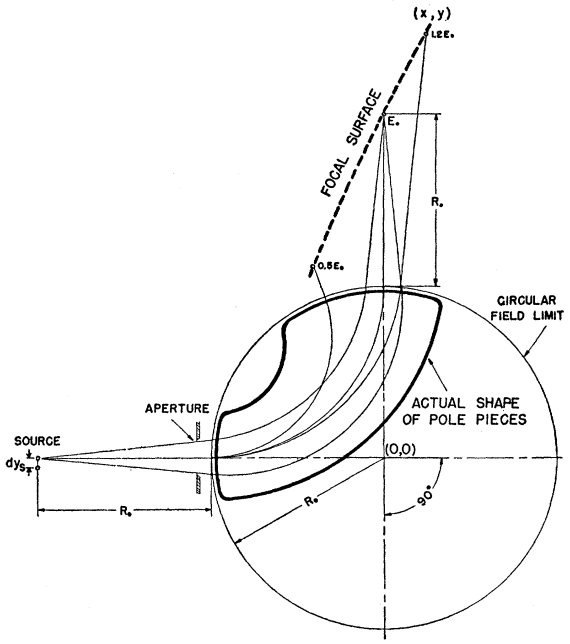

FIG. 2. Diagram showing location of source, poles, and focal surface.

II. EXPERIMENTAL ARRANGEMENT

The MIT–ONR generator, together with the associated deflecting magnet,[4] was used as a source of deuterons. For these experiments, the deflecting magnet and attached slit system was oriented so as to direct the horizontal deuteron beam into the target chamber of the new uniform field, sector-type magnetic spectrograph, as shown schematically in Fig. 1. A particular feature of this instrument is that, when nuclear-track plates are used for detection, a spectrum of protons covering a range in energy of 2.4 can be simultaneously recorded with good resolution. For this reason, we refer to the instrument as a "broad-range" spectrograph. When used in this way, the total length of plate exposed is 30 inches. For convenience in handling, three plates, each 10 in.$\times$2 in., are used. They are placed end to end in a plateholder arranged so that the long edges of the sensitized surfaces are held against a brass template shaped to correspond to the focal surface. The plateholder can be translated so that several exposures can be made on one set of plates.

The geometrical features of the spectrograph that are important for the present discussion are indicated in Fig. 2. The essential feature is that the source of particles is located a distance R_0 from the boundary of a uniform magnetic field, the entrance and exit edges of which have a radius of curvature also equal to R_0. Bainbridge has shown[5] that, with this arrangement of

[4] Buechner, Sperduto, Browne, and Bockelman, Phys. Rev. **91**, 1502 (1953).
[5] K. T. Bainbridge, *Experimental Nuclear Physics* (John Wiley and Sons, Inc., New York, 1953), Vol. 1, p. 589.

source and field, second-order focusing is achieved for particles with a radius of curvature R_0 in the field. For these particles, the source and image are symmetrically located as shown in the figure. Important for the present application is the fact that, with this geometry, the central trajectory of any other group of particles having a radius of curvature, r, different than R_0, enters and leaves the region of the field normal to the field boundary, and the other trajectories of this group are symmetrically disposed with respect to the central one. With such a symmetrical arrangement, the defocusing action of the fringing field is minimized and the allowance for the effects of fringing fields is simplified.

From Barber's rule for focusing or from the equations of ion optics,[5] it can be shown that the focal points for particles of radius of curvature, r, lie along a hyperbola, the parametric equations of which are

$$x=\frac{2R_0(r^2-R_0^2)}{3R_0^2-r^2},\quad y=\frac{4rR_0^2}{3R_0^2-r^2}. \tag{1}$$

For these equations, the origin of coordinates is at the center of curvature of the magnetic field boundary and x and y are positive in the first quadrant in the figure.

In practice, the magnetic field does not stop at the actual pole boundaries, so it is not feasible to locate the focal surface with sufficient accuracy from the analytical expressions of first-order focusing theory. The effects of the fringing field have been discussed by Bainbridge. The most important of these effects causes the magnetic field to have an effective radius somewhat larger than that of the poles. In the present case, the source was located on the assumption that the effective radius R_0 exceeded the radius of the pole (50 cm) by one gap width ($\frac{1}{2}$ inch). The focal surface was then located empirically from measurements made with nuclear-track plates and an alpha-particle source of polonium.

After the focal surface was located, the spectrograph was calibrated by measuring the positions of the group from the polonium alpha-particle source for various magnetic field strengths. This calibration gives the radius of curvature of a group of particles as a function of the location of the group on a track plate placed along the focal surface. The aberrations of the spectrograph are such that, for a monoenergetic source, the sharp edge of the peak from a group of particles lies on the low-energy side of the peak for $r>R_0$ and the high-energy side for $r<R_0$. In practice, the aberration is small, and the dispersion is such that even very small energy spreads in the source cause a measurable tail on the low-energy side of the peaks. Thus, in practice, the high-energy sides of the peaks are the sharpest and least affected by the experimental conditions, and we have used the point on this edge at one-third the maximum as a measure of the group location, both for the alpha-particle groups used for calibration and for the reaction groups to be described.

Although Eqs. (1) cannot be employed to obtain an accurate calibration, they can be used for a discussion of the dispersion and resolution of the spectrograph. From these equations, it can readily be shown that, as a result of a transverse displacement of the source by an amount dy_s (negative as shown in Fig. 2) or of a change in radius of curvature of the particles from the source by an amount dr, the image is displaced along the focal surface by an amount dS given by

$$dS=\frac{(r^2+R_0^2)(r^4+10r^2R_0^2+9r_0^4)^{\frac{1}{2}}}{(3R_0^2-r^2)^2}dy_s + \frac{4R_0^2(r^4+10r^2R_0^2+9R_0^4)^{\frac{1}{2}}}{(3R_0^2-r^2)^2}dr. \tag{2}$$

The second term of Eq. (2) enables the calculation of the dispersion of the spectrograph. Since this term depends on r, the dispersion varies with position on the plate. Since, for a given magnetic field, $dE/E=2dr/r$, the fractional change in energy of a group that will produce unit displacement along the plate is given by

$$\frac{1}{E}\frac{dE}{dS}=(3R_0^2-r^2)^2(r^4+10r^2R_0^2+9R_0^4)^{-\frac{1}{2}}/2rR_0^2. \tag{3}$$

This expression is essentially the reciprocal of the usual dispersion. For the present work, however, it is more convenient to express the dispersion in the form

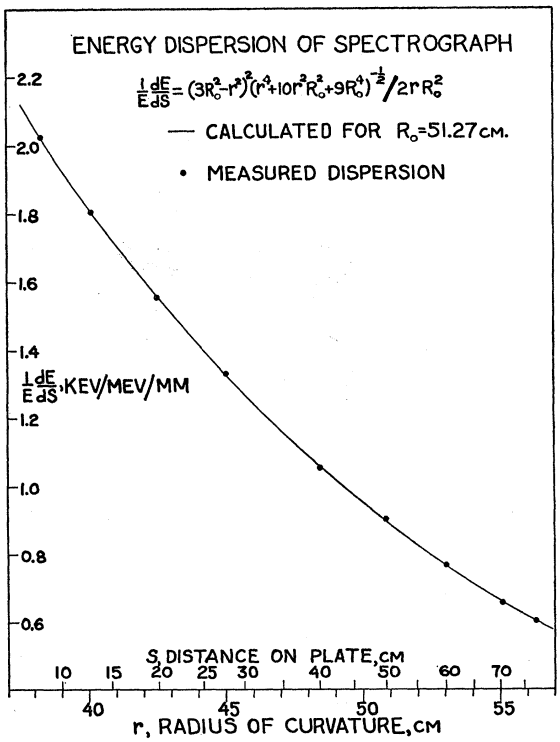

FIG. 3. Dispersion of spectrograph as a function of position along the focal surface.

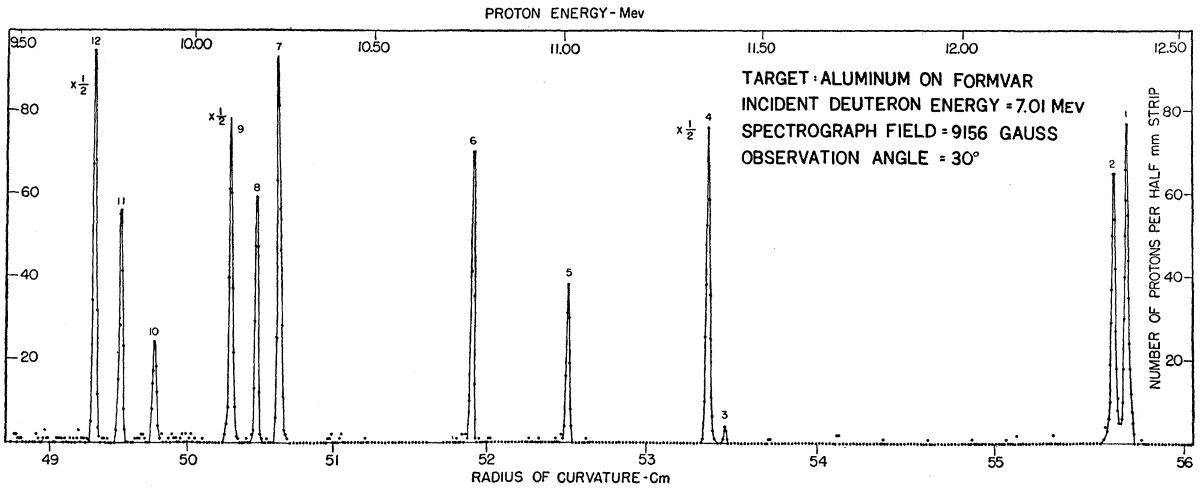

FIG. 4. High-energy proton groups from the $Al^{27}(d,p)Al^{28}$ reaction. The ground-state group is marked number 1.

of Eq. (3), and this quantity, expressed in units of kev/Mev/mm, has been calculated on the assumption that R_0 is equal to the pole radius plus one gap width (51.27 cm); the resulting curve is plotted in Fig. 3. The distances along the plate S, corresponding to given values of r, as determined from the calibration, are marked along the axis of r. The dispersion can also be determined directly from the experimental calibration, and representative points thus obtained are also shown in Fig. 3. The good agreement between the experimental points and the calculated curve indicates that the results from the first-order theory may be applied with an accuracy sufficient for the present purpose. Since the resolution achieved in practice depends on other factors in addition to the spectrograph geometry, it will be discussed later in connection with the experimental results on the $Al(d,p)$ reaction.

The angular spread in the vertical plane of the particles accepted by the spectrograph is determined by an aperture at the entrance to the spectrograph, as shown in Fig. 2. For the present work on the closely spaced groups from aluminum, where it was desirable that the effects of spectrograph aberrations be small compared with those caused by energy spread in the deuteron beam and by target thickness, this angular spread was limited to 1.5 degrees. During most of this investigation, the angular spread in the horizontal plane was limited by an 8-mm wide slit placed immediately in front of the plate. The angle subtended by this aperture varied with position along the plate, but for no position was it greater than $\frac{1}{2}$ degree. For the groups of interest in this experiment, neither angular spread was significant in its effect on the peak shape. However, for groups arising from light contaminants, the dispersion was such that, because of the rapid variation of the energies of these groups with the angle of observation, the peaks were found to be noticeably slanted across the 8-mm wide strip of exposed emulsion.

The magnetic fields in both the deflecting magnet and the spectrograph were measured with nuclear magnetic resonance fluxmeters. The exciting current for each magnet was supplied by electronically stabilized, three-phase rectifiers constructed by H. Enge. To take full advantage of the dispersion of the spectrograph, the magnetic fields must be constant to a high degree during an exposure, and these circuits have been exceedingly satisfactory.

The bombarding energies for the individual exposures were determined from measurements with the spectrograph on particles elastically scattered from the various nuclei in the targets used. The good agreement between the Q-values found in the present work for the various proton groups from carbon, nitrogen, and oxygen present on the targets as contaminants and those measured[6] in our 180-degree magnetic spectrograph indicated that the calibration procedure was sufficiently accurate for the purposes of this experiment.

The targets used consisted of a thin layer of aluminum evaporated onto a formvar film. Beam currents from 0.1 to 1 microampere were used during the course of the experiment. In all the exposures, the beam was incident on the aluminum side of the target. In the exposures at 90 degrees to the incident beam, the emergent protons were observed from the side of the target surface struck by the beam; while, for the exposures made at forward angles, the protons observed had passed through the formvar backing. In the exposures for the proton groups, aluminum foils of sufficient thickness to stop alpha particles and deuterons were placed immediately in front of the nuclear-track plates.

III. RESULTS

A number of exposures at various deuteron energies and angles of observation were made in order to study

[6] Sperduto, Buechner, Bockelman, and Browne, Phys. Rev. **96**, 1316 (1954).

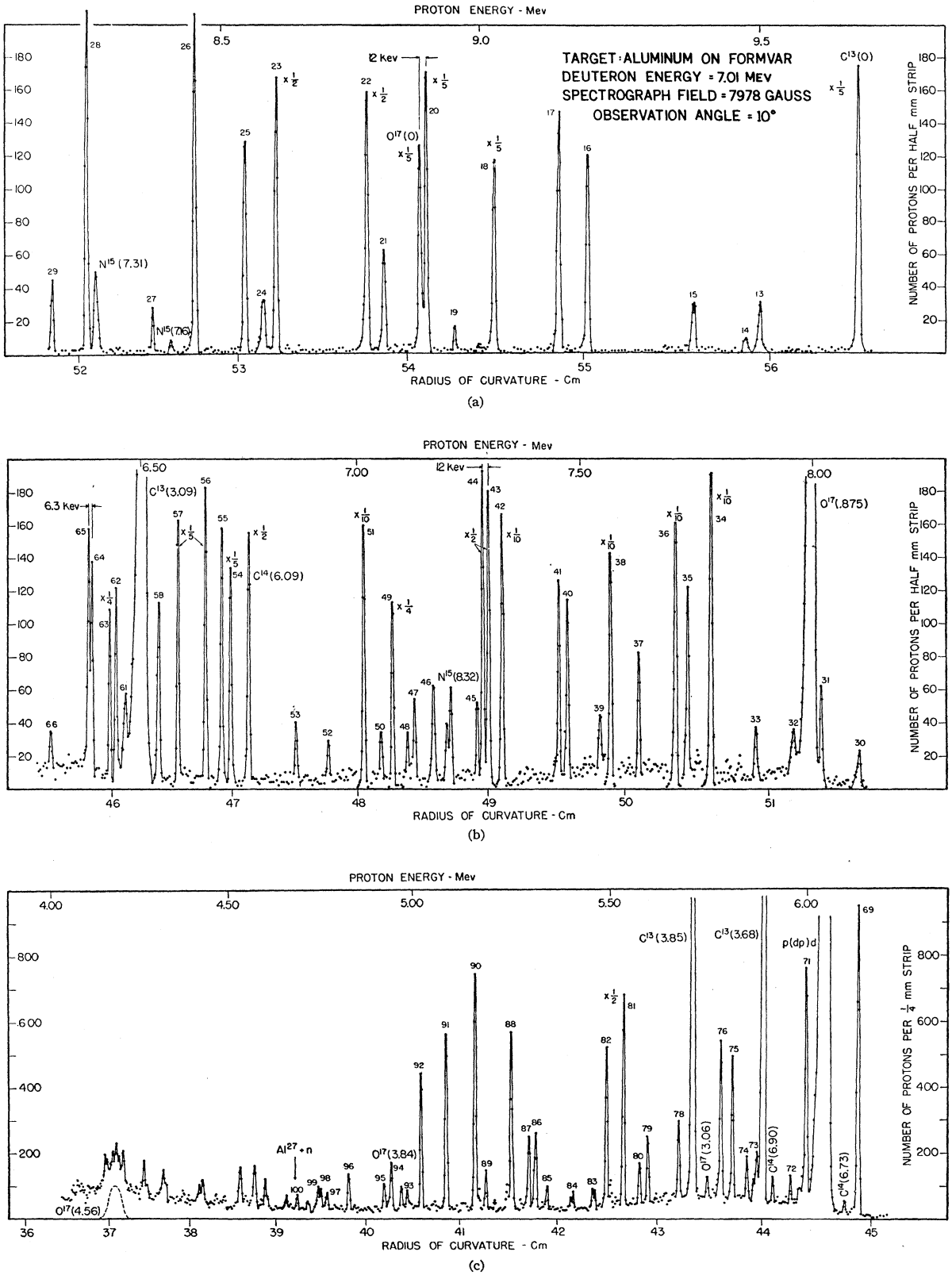

FIG. 5. Lower energy proton groups from $Al^{27}(d,p)Al^{28}$. Data from a single 600-microcoulomb exposure.

the region of excitation in Al^{28} covered in the earlier work.[3] With the broad-range spectrograph, it was possible to record simultaneously all the groups previously investigated. Analysis of the plates showed that, in the region of excitation in Al^{28} up to 3 Mev, the present results agreed in detail with those obtained at 90 degrees at the lower bombarding energy, both as to the number of groups and their Q-values. In this region, there are twelve proton groups, as shown in Fig. 4, which is a plot of the data obtained from the high-energy portion of a plate exposed at 7 Mev and 30 degrees to the beam. Similar plots, but with differing relative intensities, were obtained from the other exposures. The experimental angular distribution curves for these twelve groups have been published.[2]

It was apparent from these exposures that in the region of proton energies corresponding to excitation energies in Al^{28} greater than 3 Mev, a number of groups appeared which were not observed in the earlier experiments. In order to study this region in more detail, several exposures were made with the spectrograph field such that the thirteenth most energetic proton group (group $G1$ in the earlier work) was near the high-energy end of the plates. Such exposures were made at 90 degrees to the beam with deuteron energies of 6 and 7 Mev and at 10 degrees with 7-Mev bombarding energy. A plot of the proton spectrum recorded with a 600-microcoulomb exposure taken at 10 degrees to the beam is shown in Figs. 5(a), 5(b), and 5(c). Similar data were obtained from the other exposures.

The exposed plates were examined with a microscope. In the case of the less intense groups, the data recorded were the number of protons per half-mm wide strip as a function of position of the strip along the plate. The more intense groups were counted in strips one-quarter mm wide. In each case, the strips were 8-mm long, the full width of the exposed portion of the emulsion. In Figs. 4, 5(a), and 5(b), all the groups were normalized to a one-half mm strip width. All the data in Fig. 5(c) were obtained with a one-quarter mm strip width. In comparing relative intensities of the groups, it should be noted that Fig. 5(c) also has a different vertical scale. Since all parts of the plate are not at the same distance from the target, the intensity of a given group as observed depends on its position on the plate. This leads to a variation in the effective solid angle along the plate, the variation being approximately linear and such that the ratio of the solid angle at a radius of curvature of 37 cm to that at a radius of 56 cm is 1.5. It should also be noted that many of the groups in Figs. 4 and 5 are plotted to a reduced scale, as indicated by the fractions near the peaks. The absence of appreciable low-energy background from the intense groups is gratifying. Such background is often produced by various scattering processes and tends to obscure low-intensity groups.

Several of the observed groups were identified, from their Q-values and from the manner in which their energy varied with angle and bombarding energy, as arising from carbon, oxygen, and nitrogen. These groups are identified in the figures according to the residual nucleus formed in the (d,p) reaction involving them; the accompanying figures give the excitation energy of the corresponding residual nucleus. Several of these groups from contaminants were so intense as to be uncountable and indeed showed as visible lines on the plates. Short exposures were made to reduce these groups to countable intensities. A particularly intense group was produced by hydrogen ions driven from the target by the incident beam. This group appears with an energy of 6 Mev in Fig. 5(c) and is responsible for much of the background at lower energies. The local regions obscured by these contaminant groups and the regions near the plate edges were studied in the plates taken at other angles.

As has been mentioned, one of the purposes of this investigation was the determination of the resolution in energy which could be achieved in practice with the spectrograph. This resolution depends both on the dispersion and on the peak widths. These widths and the detailed peak shapes depend on a number of factors, the most important of which are:

(1) Energy spread in the particles emitted from the target, caused either by the target thickness or by an energy spread in the bombarding beam;

(2) Size of the bombarded area on the target and the linear magnification of the spectrograph;

(3) Drifts in the magnetic field during an exposure;

(4) Displacement of the track plate from the true focal surface;

(5) Aberrations of the spectrograph;

(6) The width of the strips used in counting the number of tracks as a function of position along the plates; and

(7) The relative widths of the beam from the deflecting magnet before and after passing through the final exit slit which defines the size and location of the bombarded area of the target.

The importance of the last factor can be seen from Eq. (2). Both dy_s and dr are influenced by the slit width. If the slit width is small compared to the beam size, the possible variation of energy of the bombarding particles and the resulting dr for the particles emitted from the target are essentially independent of the slit width and of dy_s. If, on the other hand, the beam width is small compared with the slit opening, the value of dr associated with a particular point on the target is proportional to the corresponding dy_s and is opposite in sign. In the exposures for Figs. 4 and 5, where a one-quarter mm slit was used, the first of these two limiting possibilities was more nearly realized. The other factors listed all tend to increase the peak width and, hence, to decrease the resolution. In the present experiment, factors 1 and 2 were the most important.

The large number of groups in Fig. 5 make this exposure a suitable one for determining the resolution

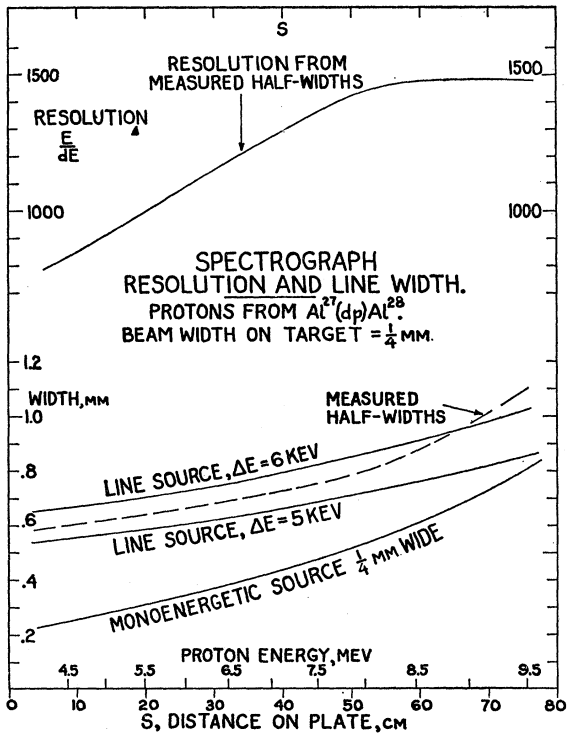

FIG. 6. Resolution and line width. The measured half-widths are those of the groups in Fig. 5.

for a wide range of particle energies. The full widths at half-maximum of 60 of the most intense groups in Fig. 5 were measured. Within the accuracy of the measurement, which was about 0.1 mm, these measured widths varied smoothly when plotted as a function of peak position. The dashed curve in Fig. 6 shows this variation in half-width with position on the plate. The track distributions in each peak were approximately triangular and a usual convention is that two such peaks are just resolved if their separation is equal to their half-width. The resolution is measured by E/dE, where E is the energy of the group and dE is the half-width expressed in energy units. The resolution calculated in this way from the half-widths shown by the dashed curve is plotted in the upper part of Fig. 6. That this definition of resolution is meaningful in the present case can be seen from Fig. 5, where the energy separation of several closely spaced groups is indicated. Since all these groups were recorded simultaneously, it is significant that three of the low-intensity groups in Fig. 5(a) had a half-width distinctly greater than the average. Whether these groups actually have unresolved components is at present uncertain. With these three exceptions, all the groups appear single within the present resolution.

The curve in Fig. 6 shows that for most of the groups in Fig. 5 the resolution was between 1000 and 1500. This is considerably less than the resolution of which the spectrograph is capable, as has been shown by tests with very thin polonium sources. The factors that limit the resolution in the present work are indicated in Fig. 6. From Eq. (2), the widths along the plate of the traces from line sources having energy spreads of 5 and 6 kev have been calculated as well as the width to be expected from a monoenergetic source having the same dimension as the bombarded area on the target. These calculated widths are shown in Fig. 6. While no detailed calculation of resultant line shape has been made, it appears that an energy spread of 0.07% in the 7-Mev deuteron beam incident on the one-quarter mm wide bombarded area of the target would account for the observed resolution. This energy spread in the deuteron beam was quite possible with the geometry of the deflecting magnet assembly as employed in the present experiments.

TABLE I. Q-values for the $Al^{27}(d,p)Al^{28}$ reaction.

Group number	Present work $E_d=7.0$ Mev	Enge[a] $E_d=2.0$ Mev	Group number	Present work $E_d=7.0$ Mev	Enge[a] $E_d=2.0$ Mev
1	5.502	5.494	51	0.057	0.060
2	5.473	5.463	52	−0.023	···
3	4.485	4.481	53	−0.094	···
4	4.529	4.521	54	−0.244	−0.241
5	4.130	4.128	55	−0.264	−0.261
6	3.869	3.873	56	−0.300	−0.298
7	3.359	3.359	57	−0.365	−0.361
8	3.295	3.298	58	−0.407	···
9	3.223	3.228	59	−0.429	···
10	3.012	3.012	60	−0.458	···
11	2.913	2.917	61	−0.487	···
12	2.839	2.843	62	−0.510	···
13	2.514	2.513	63	−0.525	−0.519
14	2.491	2.487	64	−0.565	···
15	2.400	···	65	−0.571	···
16	2.208	2.202	66	−0.661	···
17	2.155	2.152	67	−0.699	−0.693
18	2.041	2.034	68	−0.745	···
19	1.965	1.961	69	−0.820	−0.813
20	1.911	1.907	70	−0.922	···
21	1.833	1.828	71	−0.944	···
22	1.798	1.796	72	−0.983	···
23	1.624	1.621	73	−1.067	···
24	1.602	1.595	74	−1.089	···
25	1.567	1.563	75	−1.124	···
26	1.472	1.464	76	−1.155	···
27	1.387	1.383	77	−1.217	···
28	1.259	1.256	78	−1.258	···
29	1.187	1.186	79	−1.333	···
30	1.119	···	80	−1.354	···
31	1.036	1.039	81	−1.394	···
32	0.984	0.982	82	−1.432	···
33	0.907	···	83	−1.468	···
34	0.817	0.808	84	−1.523	···
35	0.761	0.758	85	−1.588	···
36	0.735	0.735	86	−1.619	···
37	0.657	0.653	87	−1.647	···
38	0.596	0.596	88	−1.678	···
39	0.574	···	89	−1.745	···
40	0.503	0.506	90	−1.772	···
41	0.483	0.486	91	−1.843	···
42	0.364	0.366	92	−1.906	···
43	0.334	0.337	93	−1.942	···
44	0.323	0.324	94	−1.958	···
45	0.311	0.312	95	−2.003	···
46	0.213	···	96	−2.094	···
47	0.171	···	97	−2.153	···
48	0.156	···	98	−2.167	···
49	0.125	0.124	99	−2.198	···
50	0.097	···	100	−2.229	···

The relative importance of such an energy spread on the resolution decreases with increasing proton energy. Thus, the higher energy groups shown in Fig. 4 should show a somewhat increased resolution. Actually, the exposure for Fig. 4 was made with a thicker target than was used for Fig. 5, and consequently the half-widths of these higher energy groups are nearly constant. The resolution for the ground-state group at the right of Fig. 4 is thus only 1600.

From these results, it appears that, while special precautions will be required to utilize fully the resolution of which the spectrograph is capable, a resolution of between 1000 and 1500 is quite practical in routine work with this instrument.

The Q-values of the groups from aluminum in Figs. 4 and 5 have been calculated, and the values are listed in Table I, together with those obtained by Enge *et al.*[3] using 2-Mev deuterons. For the reasons mentioned previously, most of this work has been concerned with the groups shown in Fig. 5. The Q-values for the first twelve groups are those obtained from the single exposure of Fig. 4. The Q-values of all the other groups listed in the table have been obtained from at least three different exposures at various energies or angles, except in a few cases where, because of intense contaminant groups, only two measurements have been used for identification purposes. Of the one hundred groups listed, only six (Numbers 59, 60, 67, 68, 70, and 77) are not shown in Fig. 5. These are either obscured by contaminant groups or fall in the region between the plates for the spectrum shown in the figure. These groups were observed at the other angles and bombarding energies. With only a few exceptions, the Q-values calculated for various bombardments at different angles and energies differ by 5 kev or less from the values listed in the table. In no case were these differences greater than 10 kev. Studies of deuterons elastically scattered from the targets used indicate that only carbon, oxygen, and nitrogen were present as contaminants in significant amount.

The proton groups in Fig. 5(c) with energies less than 4.67 are associated with the formation of Al^{28} in states which are unstable with respect to neutron emission. This energy is indicated on the figure. Such states may show a natural width large enough to be measured, and it is clear in the figure that in this region there is evidence for a number of overlapping groups. An adequate investigation of these groups would require higher resolution of the deuteron beam than was used in the present experiments, and accurate Q-values have not been calculated for the groups in this region. There is approximate agreement between the positions of these groups and the apparently unresolved resonances found by Henkel and Barschall[7] in studies of neutron scattering from aluminum. The complex structure at 37-cm radius of curvature appears to be a result of a superposition of a number of groups from aluminum onto the broad proton group associated with the formation of the 4.56-Mev level in O^{17}. This group, which arises from $O^{16}(d,p)O^{17}$, has a width of approximately 35 kev, and its expected location and shape are shown as a dashed curve in the figure.

In Table I, it is seen that all the groups found in the previous investigation[3] have also been observed in the present work. In addition, in the region of excitation in Al^{28} above 3 Mev, numerous additional groups have appeared which were not observed in the earlier work, presumably because of the lower bombarding energy used. The region of excitation above 6.3 Mev was not studied in the previous work, and so no comparison of these new Q-values is possible. Up to this point, however, the agreement with the older values is satisfactory. There is a slight but noticeable trend in the differences between the present Q-values and the older ones. This difference, for the Q-values obtained from a particular exposure, tends to increase with increasing proton energy. This trend is probably a result of a suspected slight displacement of the target spot from the location of the polonium source used for calibration and of the fact that in the present work the entrance aperture of the spectrograph was smaller than was the case for the calibration exposures. Both these effects would act in a direction to give the observed trend. However, the differences between the two sets of Q-values is within the experimental errors which were approximately ± 10 kev in each case. In Table I, it may be noted that there are slight differences between the values of the earlier Q-values listed and those in reference 3. The values listed result from a recent recalculation of the earlier data, taking into account various small correction terms.[8]

We wish to thank our colleagues in the Laboratory for their cooperation during the course of this investigation and Mr. W. A. Tripp for his careful reading of the many plates. We are indebted to the National University of Mexico, the Cultural Interchange Office of the U. S. Department of State, and Ingenieros Civiles Asociados for support to one of us (M. M.).

[7] R. L. Henkel and H. H. Barschall, Phys. Rev. **80**, 145 (1950).
[8] H. A. Enge, Univ. i Bergen Arbok, Naturvitenskap. Rekke. No. 1 (1953).